Published in final edited form as:
J Alzheimers Dis. 2010 ; 20(1): 333–341. doi:10.3233/JAD-2010-1368.

Prevalent Iron Metabolism Gene Variants Associated with Increased Brain Ferritin Iron in Healthy Older Men

George Bartzokis[a,b,c,*], **Po H. Lu**[d], **Todd A. Tishler**[a,c], **Douglas G. Peters**[a,c], **Anastasia Kosenko**[a,c], **Katherine A. Barrall**[a], **J. Paul Finn**[e], **Pablo Villablanca**[e], **Gerhard Laub**[f], **Lori L. Altshuler**[a,c], **Daniel H. Geschwind**[d], **Jim Mintz**[g], **Elizabeth Neely**[h], and **James R. Connor**[h]

[a]Department of Psychiatry and Biobehavioral Sciences and Semel Institute, The David Geffen School of Medicine at UCLA, Los Angeles, CA, USA

[b]Laboratory of Neuroimaging, Department of Neurology, Division of Brain Mapping, UCLA, Los Angeles, CA, USA

[c]Greater Los Angeles VA Healthcare System, West Los Angeles, CA, USA

[d]Department of Neurology, The David Geffen School of Medicine at UCLA, Los Angeles, CA, USA

[e]Department of Radiology, The David Geffen School of Medicine at UCLA, Los Angeles, CA, USA

[f]Siemens Medical Solutions, Los Angeles, CA, USA

[g]University of Texas Health Science Center at San Antonio, Department of Epidemiology and Biostatistics, San Antonio, TX, USA

[h]Department of Neurosurgery, Penn State Hershey Medical Center, Hershey, PA, USA

Abstract

Prevalent gene variants involved in iron metabolism [hemochromatosis (HFE) H63D and transferrin C2 (TfC2)] have been associated with higher risk and earlier age at onset of Alzheimer's disease (AD), especially in men. Brain iron increases with age, is higher in men, and is abnormally elevated in several neurodegenerative diseases, including AD and Parkinson's disease, where it has been reported to contribute to younger age at onset in men. The effects of the common genetic variants (HFE H63D and/or TfC2) on brain iron were studied across eight brain regions (caudate, putamen, globus pallidus, thalamus, hippocampus, white matter of frontal lobe, genu, and splenium of corpus callosum) in 66 healthy adults (35 men, 31 women) aged 55 to 76. The iron content of ferritin molecules (ferritin iron) in the brain was measured with MRI utilizing the Field Dependent Relaxation Rate Increase (FDRI) method. 47% of the sample carried neither genetic variant (IRON−) and 53% carried one and/or the other (IRON+). IRON+ men had significantly higher FDRI compared to IRON− men ($p = 0.013$). This genotype effect was not observed in women who, as expected, had lower FDRI than men. This is the first published evidence that these highly prevalent genetic variants in iron metabolism genes can influence brain iron levels in men. Clinical phenomena such as differential gender-associated risks of developing neurodegenerative diseases and age at onset may be associated with interactions between iron

[*]Correspondence to: George Bartzokis, M.D., 300 UCLA Medical Plaza, Suite 2200, Los Angeles, CA 90095-6968, USA. Tel.: +1 310 206 3207; Fax: +1 310 268 3266; gbar@ucla.edu.

Authors' disclosures available online (http://www.j-alz.com/disclosures/view.php?id=254.

genes and brain iron accumulation. Clarifying mechanisms of brain iron accumulation may help identify novel interventions for age-related neurodegenerative diseases.

Keywords

Alpha synuclein; amyloid; basal ganglia; chelation; dementia; diet; free radicals; gene; gray matter; iron; Lewy body; metal; myelin; oligodendrocytes; prevention; risk; tau; treatment

INTRODUCTION

Although essential for cell function, increased tissue iron can promote tissue oxidative damage to which the brain is especially vulnerable (for review see [1–5]). Human brain has a higher concentration of iron compared to other species ([6], reviewed in [7]). In human brain, iron may contribute to the development of abnormal protein deposits that are pathognomonic for several prevalent age-related neurodegenerative diseases such as Alzheimer's disease (AD), Parkinson's disease (PD), and Dementia with Lewy Bodies (DLB) (for review see [1,3,4,6–9]). Brain iron levels increase with age [10–15] and are abnormally elevated in age-related neurodegenerative diseases, suggesting that increased iron levels may contribute to their increasing prevalence with age (for review see [1,3,4,7–9]).

We recently demonstrated increased brain iron levels in men compared to women [15] and that elevated brain iron levels may contribute to the risk of developing neurodegenerative diseases at earlier ages in men [16]. Men are at higher risk of developing PD than women and with earlier age of onset [17,18]. Men are also more likely to develop extrapyramidal (motor) side effects when treated with dopaminergic agents, suggesting an elevated susceptibility of their basal ganglia to toxicity (reviewed in [19]). Extrapyramidal symptoms are a core diagnostic feature of DLB, the second most common dementia after AD [20]. Like PD, DLB also has a male predominance [20] especially in individuals with younger age at onset (under age 70) [20]. Males also have a higher risk of developing AD at younger ages [21–23].

Epidemiologic studies suggest that highly prevalent gene variants involved in iron absorption, transport, and metabolism could influence the age at onset of AD ([24–27], reviewed in [28], but see [29]). The presence of the hemochromatosis (HFE) gene variants (H63D and C282Y) increases peripheral iron load [30] as well as affecting brain tissue iron metabolism (reviewed in [1]), and it has been associated with higher risk of developing AD in individuals with younger age at onset (before age 70) [25], especially in males [23,24], and increased oxidative stress and disease severity [31]. The H63D gene variant has also been associated with an increased risk of amyotrophic lateral sclerosis (ALS) [32], can alter protein profiles in the cerebrospinal fluid (CSF) of individuals with this disease [33], and may also be associated with other neurodegenerative disorders [32,34,35]. Transferrin is also crucial for iron metabolism and brain development and repair (reviewed in [1,2,15,36]). Interactions of HFE genes with the transferrin C2 (TfC2) gene variant have also been reported to potentiate risk of developing AD and prompted calls for *in vivo* assessments of brain iron in carriers and non-carriers of these very common genetic variants [5,27]. Herein we present the first such study.

Brain iron levels can be measured *in vivo* using magnetic resonance imaging (MRI) through the effect of iron on transverse relaxation rates (R_2) [13,37,38]. The bulk of brain iron is stored in ferritin molecules [39,40], and an *in vivo* MRI method called field-dependent R_2 increase (FDRI) can obtain specific measures of the iron content of ferritin molecules

[7,13,37]. The method takes advantage of the fact that ferritin increases R_2 linearly with the field strength of the MRI instrument to produce a highly specific and reproducible measure of this tissue iron store [7,13,37] and has been shown to be elevated in AD, PD, and Huntington's disease (HD) [19,41,42].

Briefly, FDRI is the difference in measures of brain R_2 obtained with two different field-strength MRI instruments. In the presence of ferritin, R_2 increases with increasing magnetic field-strength [13,14,37,38,43–45]. This field-dependent R_2 increase is specifically associated with total iron content of ferritin molecules [37,38] and is independent of the amount of iron loading (number of iron atoms per molecule of ferritin) [45]. Thus, FDRI is a specific measure of the total iron contained in ferric oxyhydroxide particles that form the mineral core of ferritin molecules. In human tissue, ferritin and its breakdown product (hemosiderin) are physiologic sources of such particles [37,38,43,46]. The FDRI measure will therefore be referred to herein as ferritin iron [19,41].

We tested the hypothesis that over their lifetime, even *healthy older* carriers of the HFE and/or TfC2 variants (IRON+) would accumulate more brain ferritin iron than non-carriers (IRON−). Based on data that men have higher brain iron [7], develop neurodegenerative diseases at younger ages [16–22], and that in women brain iron may be affected by gender-specific life events such as hysterectomy (unpublished data), we hypothesized that the relationship between brain ferritin iron and genes would be most prominent in men.

METHODS

The subjects and methods were described previously [15] and are summarized here.

Subjects

Normal adult volunteers participating in the study were recruited from the community and hospital staff for a study of healthy aging. Potential subjects were excluded if they had a history of neurological disorder or a family history of AD or other neurodegenerative disorder, psychiatric illness (including drug or alcohol abuse), or head injury resulting in loss of consciousness for more than 10 minutes. The subjects were physically very healthy and were excluded if they were obese, or if they had a current or prior serious illness. They were independently functioning and had no evidence of neurocognitive impairment or gross neurological abnormalities on clinical interview and brief neurological examination with the study PI. The final population of 66 individuals contained 35 males and 31 females ranging in age from 55 to 76 years (mean= 66.7 years, SD = 6.1). The sample averaged 15.8 years of education (SD = 2.5; range = 12–23 years) and the racial composition was comprised of 48 (73%) Caucasian, 13 (20%) Asian, and 5 (7%) African-American subjects.

The participants were first evaluated with MRI (scanned using two MR instruments (1.5 and 0.5T) within 1 hour of each other using the same imaging protocol) and were later genotyped for the presence of hemochromatosis (HFE) and transferrin (TfC2) genes. Thirty-five subjects have one or both iron absorption genes (IRON+ group; 20 males, 15 females) while 31 have neither gene (IRON− group; 15 males, 16 females). Twenty-four percent of the total sample carried the HFE H63D variant and 38% carried the TfC2 variant. There were no carriers of the rare HFE C282Y variant in this sample.

MRI protocol

The methods have been previously described in detail [13,15,37]. Coronal and sagittal pilot scans were first obtained to specify the location and spatial orientation of the head and the position of the axial image acquisition grid. The axial image acquisition sequence acquired interleaved contiguous slices using a Carr Purcell Meiboom Gill dual spin-echo sequence

[time to repetition (TR) = 2500 msec; time to echo (TE) = 20 and 90 msec; 2 excitations; 3 mm slice thickness; 192 gradient steps; and 25 cm field of view]. The coronal and sagittal pilot scans were used to determine the alignment and accuracy of head repositioning in the second MRI instrument [13,37].

Data for each region of interest (ROI) (depicted in Fig. 1) were obtained from contiguous pairs of slices. The slice containing the anterior commissure and the slice immediately superior to it were used to obtain the putamen (P) and globus pallidus (G) transverse relaxation time (T_2) data. The third and fourth slices above the anterior commissure were used to obtain the T_2 data for caudate nucleus (C) and the second and third slices superior to the orbitofrontal gray matter were used to obtain the frontal lobe white matter (Fwm) data. For the genu of the corpus callosum (Gwm), the two slices on which the angle formed by the left and right sides of the genu appeared the most linear were chosen in order to obtain a sample that would be consistently in the middle of the structure, which contains primarily fibers connecting the prefrontal cortices. For the splenium of the corpus callosum (Swm), the second and third lowest slices on which the fibers of the splenium connected in the midline were chosen in order to sample primarily the lower half of the splenium that contains predominantly primary sensory (visual) fibers. For thalamus (T), the second and third highest slices on which thalamus appears are chosen. The lateral border of the ROI is drawn along the white matter of the internal capsule using the TE = 20 image. The medial and inferior portions bordering CSF are defined using the TE = 90 image. For hippocampus (Hip), the two contiguous slices that contained the largest areas of these structures were used in the data analysis. The Hip measure was obtained from the anterior third of the structure and limited by drawing a horizontal line at the level of the cerebral peduncle to exclude any tissue posterior to that line [15].

An illustration of the *specificity* of the FDRI method for measuring iron is depicted in Fig. 1C. The T_2 weighted image is similar to a calculated T_2 measure (see image analysis section below). The thick arrows (upper right of image 1C) s how that the T_2 signal of Fwm would be darker [indicating a lower T_2 (higher R_2)] than C and P regions. This would *erroneously* suggest that C and P have *lower* iron concentrations than Fwm. The FDRI method eliminates field-independent contributions to T_2 (such as the T_2 lowering caused by the high myelin content of Fwm), resulting in the specific measure of ferritin iron that correctly shows P and C to have much higher iron levels than Fwm (see [15] for validation against post mortem data). Other field-independent effects having an opposite effect are also common when tissue damage (as observed in aging and disease) occurs. Tissue damage would increase tissue water content (e.g., edema), *raising* T_2 (lowering R_2) and in effect would mask (cancel out) T_2 reductions due to iron. This would grossly underestimate iron content and may be a key reason for the failure of some MRI studies to detect iron increases associated with neurodegenerative diseases (reviewed in [41,42]).

Image analysis

Transverse relaxation times (T_2) were calculated for each voxel from the two signal intensities (TE = 20 and 90) of the dual spin-echo sequence to produce gray-scale encoded T_2 maps of the brain [13]. The T_2 measures were extracted using an Apple Macintosh-configured image analysis workstation. T_2 data for each of the ROIs were obtained from contiguous pairs of slices. The relaxation rate (R_2) was calculated as the reciprocal of T_2 × 1000 milliseconds/second.

T_2 is a “time” (in milliseconds) and R_2 is a “rate” (per second), and these are inversely related:

$$R_2 = \frac{1000}{T_2}$$

The average R_2 of the two slices from both hemispheres were the final measures used in the subsequent analyses. The FDRI measure was calculated as the difference in R_2 (high field R_2 – low field R_2). Test-retest reliability for FDRI measures was very high with intra-class correlation coefficients ranging from 0.88 to 0.99 ($p < 0.0023$) [13,37].

Data analyses

In order to simultaneously examine the FDRI for all eight brain regions together and to control for multiple comparisons, a multivariate analysis of covariance (MANOVA) was conducted with FDRI as the dependent variable and the iron absorption gene (presence [IRON+] or absence [IRON−] of genes) and gender as the independent variables. The p-values for the MANOVA were assessed as significant at unadjusted $p = 0.05$. Post hoc comparisons using pairwise t-tests were then performed to determine the exact nature of the difference between groups. Age was not significantly different between the two groups (IRON+: mean age = 67.2, sd = 6.1; IRON−: mean age = 66.3, sd = 6.1; $t = 0.60$, df = 64, $p = 0.55$). In this restricted 20-year age span, age was also not significantly correlated with FDRI in any of the eight regions and was therefore not introduced as a covariate in subsequent analyses. The small sample size did not allow meaningful assessment of the individual contribution of the two gene variants and their combined effects due to their small cell sizes (see Table 1).

RESULTS

When the genders were combined into a single sample, the MANOVA model did not indicate an overall effect of the genotype on brain iron levels (Wilks' Lambda = 0.849, $F = 1.22$, $p = 0.304$). As expected from our previous findings involving the larger parent sample [15], a significant gender effect was observed (Wilks' Lambda = 0.755, $F = 2.23$, $p = 0.039$) with the men possessing higher FDRI. Post hoc comparisons showed the differences to be significant in frontal lobe white matter ($p = 0.028$) and thalamus ($p = 0.002$). We also observed the predicted interaction between iron gene and gender was at the trend level of significance (Wilks' Lambda=0.782, $F = 1.92$, $p = 0.075$). We therefore performed the MANOVA on each gender separately.

A significant effect of iron genes on brain ferritin iron was detected in men (Wilks' Lambda=0.510, $F = 3.12$, $p = 0.013$). This effect remains significant even when the Bonferroni correction is applied for the multiple comparison of assessing the genders separately. Post hoc comparisons revealed that the IRON+ men had significantly higher FDRI levels than IRON− men in the caudate ($p = 0.034$) with a trend in the splenium of the corpus callosum ($p = 0.061$); this group also had numerically higher FDRI in genu and putamen but not the other regions (see Table 2). There were no significant differences in the FDRI measure between IRON+ and IRON− groups of women (Wilks' Lambda=0.826, $F = 0.58$, $p = 0.784$).

DISCUSSION

The common genetic variants involved in iron absorption and metabolism (HFE and TfC2) have been reported to potentiate the risk of developing AD ([5,27], reviewed in [28]). These data prompted calls for *in vivo* assessments of brain iron in gene carriers and non-carriers

[27]. Herein we demonstrate for the first time that presence of these prevalent genetic variants is associated with brain iron levels in men.

The iron-increasing effect of these genes was not observed in women. In women, the relationships between gene and brain iron may be masked/obscured by reproduction-associated differences in iron needs, iron loss, or iron metabolism, which do not affect men ([15,47], Bartzokis et al. unpublished data). We previously reported gender differences in brain iron (higher in men) in 165 healthy adults across the age-span (19–82 years of age) [15]. The current subsample of older individuals was derived from this larger sample. The current data suggest that gender differences in brain iron may be driven in part by increased levels in IRON+ males.

Men have a younger age at onset for several neurodegenerative conditions including PD [17,18], DLB [20], and AD ([21–23], reviewed in [15]). We previously proposed that a portion of the earlier age at onset of neurodegenerative diseases such as AD, PD, and DLB in males may be accounted for by brain ferritin iron levels that are elevated in males [15,16]. We now suggest that male carriers of the HFE and TfC2 variants (approximately 50% of males in this sample) may be at an especially increased risk. The influence of these genes may be especially prominent in presymptomatic stages of the disease [25,27]. Thus, similar to the effect of apolipoprotein E4 alleles that primarily reduce the age at onset of AD [22], HFE and TfC2 mutations may manifest primarily as earlier age at onset [25], especially in men [3,16,23,24]. This possibility is also supported by recent data showing increased CNS iron levels in *preclinical* stages of AD [9,48]. Intracellular iron levels may promote both production of pathologic proteins (reviewed in [1,5,49]) as well as their oligomerization [50,51] supporting suggestions that abnormal protein aggregations and their cytotoxic effects in general may be dependent on transition metals such as iron (for review see [3,9,15]). Reducing brain iron accumulations in old age may be a modifiable risk factor for age-related neurodegenerative diseases [15]. It remains to be determined what interventions are capable of safely reducing brain iron or combating its deleterious effects [8,52–55].

One possibility is that reducing peripheral iron levels may reduce brain iron [15]. It is well established that women have lower peripheral iron levels compared to men [56,57]. There is also evidence that brain iron is responsive to peripheral iron status (for review see [58]). In this context, the gene- and gender-related differences in brain ferritin iron suggest that lower peripheral iron levels could in turn reduce brain iron levels [15]. This possibility was first noted by Hallgren and Sourander [10] based on anecdotal observations made during their landmark postmortem study of human nonheme brain iron levels. They observed that subjects with known hemorrhages or severe anemia ante mortem had lower brain iron levels at postmortem, and suggested that brain iron may be mobilized for metabolic needs outside the brain [10]. Conversely, our own preliminary data suggests that a history of hysterectomy (which would eliminate menstrual iron loss) may increase brain iron levels in healthy older women (Bartzokis, et al., unpublished data).

AD rates double every 5 years after age 60; therefore, a modifiable risk factor that delays onset by 5 years could represent a major intervention that could potentially halve the number of cases of AD. In the context of high levels of peripheral iron in the United States population (even in the elderly) [56] and the high prevalence of these iron-related gene variants [27,59], reducing peripheral iron levels could have substantial public health implications and deserves closer scrutiny [15].

Whether differences in ferritin iron reflect higher iron content per ferritin molecule as reported in some diseases like AD and PD [60,61], larger numbers of ferritin molecules, or other forms of iron particles [62,63], is not directly discernable from the FDRI data and

remains to be determined. Further limitations of this study also need to be considered. First, interpretation of gene-related differences must be made with caution in cross sectional studies [64] and prospective data are needed to further define gene-related effects on iron levels in both health and disease. Second, the small sample size did not allow meaningful assessment of the individual contribution of the two gene variants or their combined effects. Third, the absence from the sample of children, adolescents, and younger adults limits the ability to determine the age when the impact of genes is greatest and pinpoint the optimal age for intervention. Finally, although reproducible [13,41] and very highly correlated with postmortem iron levels [15], the FDRI measure specifically quantifies ferritin iron load and not the amount of free iron or other transition metals that may also be associated with toxic consequences [48,65].

Neuroimaging can assess tissue ferritin iron with specificity on a regional basis and could be used to examine the endophenotype of individuals with genetic- [24–26,32,34,35] and disease-related [66,67] markers of iron dysregulation. Neuroimaging can also be used to more precisely target emerging therapeutic interventions (for review see [8,52–55]) to high-risk groups identified by MRI, years before clinical manifestations of disease. Early intervention may make it possible to increase effectiveness of such treatments, decrease the need for later more aggressive approaches, and ultimately may represent a heretofore unexplored opportunity for primary prevention of neurodegenerative diseases [3].

Acknowledgments

This work was supported in part by NIH grants (MH0266029; AG027342; MH51928), the Department of Veterans Affairs, the RCS Alzheimer's Foundation, and the George M Leader Family.

REFERENCES

1. Zecca L, Youdim MB, Riederer P, Connor JR, Crichton RR. Iron, brain ageing and neurodegenerative disorders. Nat Rev Neurosci. 2004; 5:863–873. [PubMed: 15496864]
2. Youdim MB. Brain iron deficiency and excess; cognitive impairment and neurodegeneration with involvement of striatum and hippocampus. Neurotox Res. 2008; 14:45–56. [PubMed: 18790724]
3. Bartzokis G. Alzheimer's disease as homeostatic responses to age-related myelin breakdown. Neurobiol Aging. 2009 in press.
4. Kell DB. Iron behaving badly: inappropriate iron chelation as a major contributor to the aetiology of vascular and other progressive inflammatory and degenerative diseases. BMC Med Genomics. 2009; 2:2. [PubMed: 19133145]
5. Altamura S, Muckenthaler MU. Iron toxicity in diseases of aging: Alzheimer's disease, Parkinson's disease and atherosclerosis. J Alzheimers Dis. 2009; 16:879–895. [PubMed: 19387120]
6. Meadowcroft MD, Connor JR, Smith MB, Yang QX. MRI and histological analysis of beta-amyloid plaques in both human Alzheimer's disease and APP/PS1 transgenic mice. J Magn Reson Imaging. 2009; 29:997–1007. [PubMed: 19388095]
7. Bartzokis G, Lu PH, Mintz J. Human brain myelination and amyloid beta deposition in Alzheimer's disease. Alzheimers Dement. 2007; 3:122–125. [PubMed: 18596894]
8. Bush AI, Tanzi RE. Therapeutics for Alzheimer's disease based on the metal hypothesis. Neurotherapeutics. 2008; 5:421–432. [PubMed: 18625454]
9. Smith MA, Zhu X, Tabaton M, Liu G, McKeel DW Jr, Cohen ML, Wang X, Siedlak SL, Dwyer BE, Hayashi T, Nakamura M, Nunomura A, Perry G. Increased iron and free radical generation in preclinical alzheimer disease and mild cognitive impairment. J Alzheimers Dis. 2010; 19:363–372. [PubMed: 20061651]
10. Hallgren B, Sourander P. The effect of age on the nonhaemin iron in the human brain. J Neurochem. 1958; 3:41–51. [PubMed: 13611557]

11. Klintworth, GK. Huntington's chorea – morphologic contributions of a century. In: Barbeau, A.; Paulson, GW.; Chase, TN., editors. Advances in Neurology, v.1: Huntington's chorea, 1872–1972. New York: Raven Press; 1973. p. 353-368.
12. Hirose W, Ikematsu K, Tsuda R. Age-associated increases in heme oxygenase-1 and ferritin immunoreactivity in the autopsied brain. Leg Med (Tokyo). 2003; 5 Suppl 1:S360–S366. [PubMed: 12935634]
13. Bartzokis G, Mintz J, Sultzer D, Marx P, Herzberg JS, Phelan CK, Marder SR. In vivo MR evaluation of age-related increases in brain iron. AJNR Am J Neuroradiol. 1994; 15:1129–1138. [PubMed: 8073983]
14. Bartzokis G, Beckson MZ, Hance DB, Marx P, Foster JA, Marder SR. MR evaluation of age-related increase of brain iron in young adult and older normal males. Magn Reson Imaging. 1997; 15:29–35. [PubMed: 9084022]
15. Bartzokis G, Tishler TA, Lu PH, Villablanca P, Altshuler LL, Carter M, Huang D, Edwards N, Mintz J. Brain ferritin iron may influence age- and gender-related risks of neurodegeneration. Neurobiol Aging. 2007; 28:414–423. [PubMed: 16563566]
16. Bartzokis, G.; Tishler, TA.; Shin, I-S.; Lu, PH.; Cummings, JL. Brain ferritin iron as a risk factor for age at onset in neurodegenerative diseases. In: LeVine, S.; Connor, J.; Schipper, H., editors. Redox-active Metals in Neurological Disorders. New York: Ann N Y Acad Sci; 2004. p. 224-236.
17. Van Den Eeden SK, Tanner CM, Bernstein AL, Fross RD, Leimpeter A, Bloch DA, Nelson LM. Incidence of Parkinson's disease: variation by age, gender, and race/ethnicity. Am J Epidemiol. 2003; 157:1015–1022. [PubMed: 12777365]
18. Haaxma CA, Bloem BR, Borm GF, Oyen WJ, Leenders KL, Eshuis S, Booij J, Dluzen DE, Horstink MW. Gender differences in Parkinson's disease. J Neurol Neurosurg Psychiatry. 2006; 78:819–824. [PubMed: 17098842]
19. Bartzokis G, Cummings JL, Markham CH, Marmarelis PZ, Treciokas LJ, Tishler TA, Marder SR, Mintz J. MRI evaluation of brain iron in earlier- and later-onset Parkinson's disease and normal subjects. Magn Reson Imaging. 1999; 17:213–222. [PubMed: 10215476]
20. Barker WW, Luis CA, Kashuba A, Luis M, Harwood DG, Loewenstein D, Waters C, Jimison P, Shepherd E, Sevush S, Graff-Radford N, Newland D, Todd M, Miller B, Gold M, Heilman K, Doty L, Goodman I, Robinson B, Pearl G, Dickson D, Duara R. Relative frequencies of Alzheimer disease, Lewy body, vascular and frontotemporal dementia, and hippocampal sclerosis in the state of Florida brain bank. Alzheimer Dis Assoc Disord. 2002; 16:203–212. [PubMed: 12468894]
21. Miech RA, Breitner JC, Zandi PP, Khachaturian AS, Anthony JC, Mayer L. Incidence of AD may decline in the early 90s for men, later for women: The Cache County study. Neurology. 2002; 58:209–218. [PubMed: 11805246]
22. Raber J, Huang Y, Ashford JW. ApoE genotype accounts for the vast majority of AD risk and AD pathology. Neurobiol Aging. 2004; 25:641–650. [PubMed: 15172743]
23. Alizadeh BZ, Njajou OT, Millan MR, Hofman A, Breteler MM, van Duijn CM. HFE variants, APOE and Alzheimer's disease: Findings from the population-based Rotterdam Study. Neurobiol Aging. 2009; 30:330–332. [PubMed: 17628213]
24. Moalem S, Percy ME, Andrews DF, Kruck TP, Wong S, Dalton AJ, Mehta P, Fedor B, Warren AC. Are hereditary hemochromatosis mutations involved in Alzheimer disease? Am J Med Genet. 2000; 93:58–66. [PubMed: 10861683]
25. Sampietro M, Caputo L, Casatta A, Meregalli M, Pellagatti A, Tagliabue J, Annoni G, Vergani C. The hemochromatosis gene affects the age of onset of sporadic Alzheimer's disease. Neurobiol Aging. 2001; 22:563–568. [PubMed: 11445256]
26. Combarros O, Garcia-Roman M, Fontalba A, Fernandez-Luna JL, Llorca J, Infante J, Berciano J. Interaction of the H63D mutation in the hemochromatosis gene with the apolipoprotein E epsilon 4 allele modulates age at onset of Alzheimer's disease. Dement Geriatr Cogn Disord. 2003; 15:151–154. [PubMed: 12584430]
27. Lehmann DJ, Worwood M, Ellis R, Wimhurst VL, Merryweather-Clarke AT, Warden DR, Smith AD, Robson KJ. Iron genes, iron load and risk of Alzheimer's disease. J Med Genet. 2006; 43:e52. [PubMed: 17047092]

28. Connor JR, Lee SY. HFE mutations and Alzheimer's disease. J Alzheimers Dis. 2006; 10:267–276. [PubMed: 17119292]
29. Rondeau V, Iron A, Letenneur L, Commenges D, Duchene F, Arveiler B, Dartigues JF. Analysis of the effect of aluminum in drinking water and transferrin C2 allele on Alzheimer's disease. Eur J Neurol. 2006; 13:1022–1025. [PubMed: 16930371]
30. Burt MJ, George PM, Upton JD, Collett JA, Frampton CM, Chapman TM, Walmsley TA, Chapman BA. The significance of haemochromatosis gene mutations in the general population: implications for screening. Gut. 1998; 43:830–836. [PubMed: 9824612]
31. Pulliam JF, Jennings CD, Kryscio RJ, Davis DG, Wilson D, Montine TJ, Schmitt FA, Markesbery WR. Association of HFE mutations with neurodegeneration and oxidative stress in Alzheimer's disease and correlation with APOE. Am J Med Genet. 2003; 119B:48–53. [PubMed: 12707938]
32. Wang XS, Lee S, Simmons Z, Boyer P, Scott K, Liu W, Connor J. Increased incidence of the Hfe mutation in amyotrophic lateral sclerosis and related cellular consequences. J Neurol Sci. 2004; 227:27–33. [PubMed: 15546588]
33. Mitchell RM, Freeman WM, Randazzo WT, Stephens HE, Beard JL, Simmons Z, Connor JR. A CSF biomarker panel for identification of patients with amyotrophic lateral sclerosis. Neurology. 2009; 72:14–19. [PubMed: 18987350]
34. Demarquay G, Setiey A, Morel Y, Trepo C, Chazot G, Broussolle E. Clinical report of three patients with hereditary hemochromatosis and movement disorders. Mov Disord. 2000; 15:1204–1209. [PubMed: 11104206]
35. Dekker MC, Giesbergen PC, Njajou OT, van Swieten JC, Hofman A, Breteler MM, van Duijn CM. Mutations in the hemochromatosis gene (HFE), Parkinson's disease and parkinsonism. Neurosci Lett. 2003; 348:117–119. [PubMed: 12902032]
36. Todorich B, Pasquini JM, Garcia CI, Paez PM, Connor JR. Oligodendrocytes and myelination: The role of iron. Glia. 2009; 57:467–478. [PubMed: 18837051]
37. Bartzokis G, Aravagiri M, Oldendorf WH, Mintz J, Marder SR. Field dependent transverse relaxation rate increase may be a specific measure of tissue iron stores. Magn Reson Med. 1993; 29:459–464. [PubMed: 8464361]
38. Vymazal J, Brooks RA, Baumgarner C, Tran V, Katz D, Bulte JW, Bauminger R, Di Chiro G. The relation between brain iron and NMR relaxation times: An *in vitro* study. Magn Reson Med. 1996; 35:56–61. [PubMed: 8771022]
39. Floyd RA, Carney JM. The role of metal ions in oxidative processes and aging. Toxicol Ind Health. 1993; 9:197–214. [PubMed: 8093420]
40. Morris CM, Candy JM, Oakley AE, Bloxham CA, Edwardson JA. Histochemical distribution of non-haem iron in the human brain. Acta Anat (Basel). 1992; 144:235–257. [PubMed: 1529678]
41. Bartzokis G, Sultzer D, Cummings BJ, Holt LE, Hance DB, Henderson VW, Mintz J. In vivo evaluation of brain iron in Alzheimer's disease and normal controls using magnetic resonance imaging. Arch Gen Psychiatry. 2000; 57:47–53. [PubMed: 10632232]
42. Bartzokis G, Cummings J, Perlman S, Hance DB, Mintz J. Increased basal ganglia iron levels in Huntington disease. Arch Neurol. 1999; 56:569–574. [PubMed: 10328252]
43. Vymazal J, Hajek M, Patronas N, Giedd JN, Bulte JW, Baumgarner C, Tran V, Brooks RA. The quantitative relation between T1-weighted and T2-weighted MRI of normal gray matter and iron concentration. J Magn Reson Imaging. 1995; 5:554–560. [PubMed: 8574041]
44. Vymazal J, Brooks RA, Patronas N, Hajek M, Bulte JW, Di Chiro G. Magnetic resonance imaging of brain iron in health and disease. J Neurol Sci. 1995; 134 Suppl:19–26. [PubMed: 8847541]
45. Vymazal J, Zak O, Bulte JW, Aisen P, Brooks RA. T1 and T2 of ferritin solutions: effect of loading factor. Magn Reson Med. 1996; 36:61–65. [PubMed: 8795021]
46. Bulte JW, Miller GF, Vymazal J, Brooks RA, Frank JA. Hepatic hemosiderosis in non-human primates: quantification of liver iron using different field strengths. Magn Reson Med. 1997; 37:530–536. [PubMed: 9094074]
47. Stuckey R, Aldridge T, Lim FL, Moore DJ, Tinwell H, Doherty N, Davies R, Smith AG, Kimber I, Ashby J, Orphanides G, Moggs JG. Induction of iron homeostasis genes during estrogen-induced uterine growth and differentiation. Mol Cell Endocrinol. 2006; 253:22–29. [PubMed: 16684588]

48. Lavados M, Guillon M, Mujica MC, Rojo LE, Fuentes P, Maccioni RB. Mild cognitive impairment and Alzheimer patients display different levels of redox-active CSF iron. J Alzheimers Dis. 2008; 13:225–232. [PubMed: 18376063]

49. Rogers JT, Bush AI, Cho HH, Smith DH, Thomson AM, Friedlich AL, Lahiri DK, Leedman PJ, Huang X, Cahill CM. Iron and the translation of the amyloid precursor protein (APP) and ferritin mRNAs: riboregulation against neural oxidative damage in Alzheimer's disease. Biochem Soc Trans. 2008; 36:1282–1287. [PubMed: 19021541]

50. Frackowiak J, Potempska A, Mazur-Kolecka B. Formation of amyloid-beta oligomers in brain vascular smooth muscle cells transiently exposed to iron-induced oxidative stress. Acta Neuropathol. 2009; 117:557–567. [PubMed: 19221770]

51. Kostka M, Hogen T, Danzer KM, Levin J, Habeck M, Wirth A, Wagner R, Glabe CG, Finger S, Heinzelmann U, Garidel P, Duan W, Ross CA, Kretzschmar H, Giese A. Single-particle characterization of iron-induced pore-forming alpha-synuclein oligomers. J Biol Chem. 2008; 283:10992–11003. [PubMed: 18258594]

52. Mandel SA, Amit T, Kalfon L, Reznichenko L, Weinreb O, Youdim MB. Cell signaling pathways and iron chelation in the neurorestorative activity of green tea polyphenols: special reference to epigallocatechin gallate (EGCG). J Alzheimers Dis. 2008; 15:211–222. [PubMed: 18953110]

53. Amit T, Avramovich-Tirosh Y, Youdim MB, Mandel S. Targeting multiple Alzheimer's disease etiologies with multimodal neuroprotective and neurorestorative iron chelators. FASEB J. 2007; 22:1296–1305. [PubMed: 18048580]

54. Hider RC, Ma Y, Molina-Holgado F, Gaeta A, Roy S. Iron chelation as a potential therapy for neurodegenerative disease. Biochem Soc Trans. 2008; 36:1304–1308. [PubMed: 19021545]

55. Cahill CM, Lahiri DK, Huang X, Rogers JT. Amyloid precursor protein and alpha synuclein translation, implications for iron and inflammation in neurodegenerative diseases. Biochim Biophys Acta. 2008; 1790:615–628. [PubMed: 19166904]

56. Fleming DJ, Jacques PF, Massaro JM, D'Agostino RB Sr, Wilson PW, Wood RJ. Aspirin intake and the use of serum ferritin as a measure of iron status. Am J Clin Nutr. 2001; 74:219–226. [PubMed: 11470724]

57. Whitfield JB, Treloar S, Zhu G, Powell LW, Martin NG. Relative importance of female-specific and non-female-specific effects on variation in iron stores between women. Br J Haematol. 2003; 120:860–866. [PubMed: 12614223]

58. Beard JL, Connor JR. Iron Status and Neural Functioning. Annu Rev Nutr. 2003; 23:41–58. [PubMed: 12704220]

59. Steinberg KK, Cogswell ME, Chang JC, Caudill SP, McQuillan GM, Bowman BA, Grummer-Strawn LM, Sampson EJ, Khoury MJ, Gallagher ML. Prevalence of C282Y and H63D mutations in the hemochromatosis (HFE) gene in the United States. JAMA. 2001; 285:2216–2222. [PubMed: 11325323]

60. Griffiths PD, Dobson BR, Jones GR, Clarke DT. Iron in the basal ganglia in Parkinson's disease. An *in vitro* study using extended X-ray absorption fine structure and cryo-electron microscopy. Brain. 1999; 122:667–673. [PubMed: 10219780]

61. Fleming JT, Joshi JG. Ferritin: the role of aluminum in ferritin function. Neurobiol Aging. 1991; 12:413–418. [PubMed: 1770974]

62. Collingwood JF, Mikhaylova A, Davidson M, Batich C, Streit WJ, Terry J, Dobson J. In situ characterization and mapping of iron compounds in Alzheimer's disease tissue. J Alzheimers Dis. 2005; 7:267–272. [PubMed: 16131727]

63. Collingwood JF, Chong RK, Kasama T, Cervera-Gontard L, Dunin-Borkowski RE, Perry G, Posfai M, Siedlak SL, Simpson ET, Smith MA, Dobson J. Three-dimensional tomographic imaging and characterization of iron compounds within Alzheimer's plaque core material. J Alzheimers Dis. 2008; 14:235–245. [PubMed: 18560134]

64. Kraemer HC, Yesavage JA, Taylor JL, Kupfer D. How can we learn about developmental processes from cross-sectional studies, or can we? Am J Psychiatry. 2000; 157:163–171. [PubMed: 10671382]

65. Rajendran R, Minqin R, Ynsa MD, Casadesus G, Smith MA, Perry G, Halliwell B, Watt F. A novel approach to the identification and quantitative elemental analysis of amyloid deposits –

insights into the pathology of Alzheimer's disease. Biochem Biophys Res Commun. 2009; 382:91–95. [PubMed: 19258010]

66. Singh A, Isaac AO, Luo X, Mohan ML, Cohen ML, Chen F, Kong Q, Bartz J, Singh N. Abnormal brain iron homeostasis in human and animal prion disorders. PLoS Pathog. 2009; 5 e1000336.
67. Marques F, Falcao AM, Sousa JC, Coppola G, Geschwind D, Sousa N, Correia-Neves M, Palha JA. Altered iron metabolism is part of the choroid plexus response to peripheral inflammation. Endocrinology. 2009; 150:2822–2828. [PubMed: 19213835]

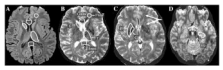

Fig. 1.

Region of interest (ROI) definition is depicted on axial MRI TE20 (image A) and TE90 (images B, C, D). The TE20 has optimal contrast between gray (appears light gray) and white matter (appears dark gray). The TE90 has optimal contrast between brain (appears gray) and CSF (appears white). Both TE20 and TE90 images are used to draw each ROI as this combination of slices maximizes contrast needed for accurate ROI definition. As an example, the use of both contrasts is depicted in the thalamus ROI that borders CSF medially and white matter laterally and posteriorly (images A and B). Data for each ROI are obtained from contiguous pairs of slices. Only one hemisphere ROI is depicted on the figures although ROIs are measured bilaterally for all regions except for midline corpus callosum regions (Gwm and Swm). **a&b:** Frontal lobe white matter (Fwm): the second and third slices superior to the orbitofrontal gray matter are chosen. A standard circular ROI template is first positioned within the desired area. The ROI is then manually edited to exclude any unwanted gray matter (which appears hyperintense) or other hyperintensities. Genu (Gwm): the two slices are chosen on which the angle formed by the left and right sides of the genu appears the most horizontal (linear). This results in a sample consistently in the middle of the structure, which contains primarily fibers connecting the prefrontal cortices. Splenium (Swm): the second and third lowest slices on which the fibers of the splenium connected in the midline are chosen. This results in a sample primarily in the lower half of the splenium, which contains predominantly primary sensory (visual) fibers. For the two corpus callosum regions (Gwm and Swm), a standard rectangular ROI template is first positioned on the midline, and then the anterior and posterior borders are manually edited to exclude non-corpus callosum tissue. Lateral borders are defined by the dimensions of the rectangular template. Caudate nucleus (C): the third and fourth slices above the anterior commissure (not shown) are chosen. Thalamus (T): the second and third highest slices on which thalamus appears are chosen. The lateral border of the ROI is drawn along the white matter of the internal capsule using the TE20 image (A). The medial and inferior portions bordering CSF are defined using the TE90 image (B). **C**: Putamen (P) and globus pallidus (G): the slice containing the anterior commissure and the slice immediately superior to it (image C) are chosen. **D**: Hippocampus (Hip): the slices containing the largest area of anterior hippocampus are chosen. The anterior Hip measure is limited posteriorly by drawing a horizontal line at the level of the cerebral peduncle to exclude any tissue below that line. The thick arrows in upper right of image C point to Fwm and P regions and are referred to in the text (see Methods section, MRI protocol, third paragraph) as an illustration of the specificity of the FDRI method.

Table 1

Study sample breakdown by gender, age, and genes

Demographic variables	**Males (*n* = 35)**				**Females (*n* = 31)**			
Age	66.5 (6.0)				67.1 (6.2)			
	IRON+ (*n* = 20)			IRON− (*n* = 15)	IRON+ (*n* = 15)			IRON− (*n* = 16)
Age	67.4 (5.9)			65.5 (6.1)	67.1 (6.5)			67.2 (6.2)
	H63D+ (*n* = 7)	H63D+/ / TfC2+ (*n* = 4)	TfC2+ (*n* = 9)		H63D+ (*n* = 3)	H63D+/ / TfC2+ (*n* = 2)	TfC2+ (*n* = 10)	

Age did not differ significantly between male and females in the overall sample ($t = 0.39$, df = 64, $p = 0.70$) or within IRON+ and IRON− groups ($p > 0.44$) or between IRON+ and IRON− subgroups ($p > 0.55$).

Table 2

Effect of iron genes on brain ferritin iron in men in individual regions

	Men age 55 and older					
	IRON+ (*n* = 20)		IRON− (*n* = 15)			
Region	**mean**	**sd**	**mean**	**sd**	**t**	**p**
C	2.71	0.42	2.36	0.52	2.21	0.034
G	4.67	0.84	4.72	0.85	−0.18	0.855
P	3.14	0.57	2.98	0.63	0.78	0.444
T	1.31	0.25	1.45	0.34	−1.36	0.184
Fwm	1.60	0.26	1.71	0.30	−1.19	0.244
Gwm	1.29	0.28	1.19	0.36	0.91	0.368
Swm	1.12	0.38	0.85	0.44	1.94	0.061
Hip	0.81	0.26	0.85	0.28	−0.40	0.691

MANOVA analysis combining all eight brain regions revealed no significant difference in women (Wilks' Lambda=0.826, $F = 0.58$, $p = 0.784$), while men showed a significant effect of iron gene carrier status on brain ferritin iron (Wilks' Lambda = 0.510, $F = 3.12$, $p = 0.013$). This table shows the post hoc t-tests for each brain region in male gene carriers (IRON+) versus non-carriers (IRON−) (df=33).

C = caudate nucleus; *G* = globus pallidus; *P* = putamen; *T* = thalamus; Fwm = frontal lobe white matter; Gwm = genu of the corpus callosum; Swm = splenium of the corpus callosum; Hip = hippocampus.